RESEARCH ARTICLE

Modeling and mapping the current and future distribution of *Pseudomonas syringae pv. actinidiae* under climate change in China

Rulin Wang[1,2☯], Qing Li[1☯]*, Shisong He[3], Yuan Liu[3], Mingtian Wang[4], Gan Jiang[2]

1 College of Agronomy, Sichuan Agricultural University, Chengdu, Sichuan, China, **2** Sichuan Provincial Rural Economic Information Center, Chengdu, Sichuan, China, **3** The Kiwifruit Institute of Cangxi Country, Cangxi, Sichuan, China, **4** Sichuan Meteorological Observatory, Chengdu, Sichuan, China

☯ These authors contributed equally to this work.
* liq8633@163.com

Abstract

Objective

Bacterial canker of kiwifruit caused by *Pseudomonas syringae pv. actinidiae* (Psa) is a major threat to the kiwifruit industry throughout the world and accounts for substantial economic losses in China. The aim of the present study was to test and explore the possibility of using MaxEnt (maximum entropy models) to predict and analyze the future large-scale distribution of Psa in China.

Method

Based on the current environmental factors, three future climate scenarios, which were suggested by the fifth IPCC report, and the current distribution sites of Psa, MaxEnt combined with ArcGIS was applied to predict the potential suitable areas and the changing trend of Psa in China. The jackknife test and correlation analysis were used to choose dominant climatic factors. The receiver operating characteristic curve (ROC) drawn by MaxEnt was used to evaluate the accuracy of the simulation.

Result

The results showed that under current climatic conditions, the area from latitude 25° to 36°N and from longitude 101° to 122°E is the primary potential suitable area of Psa in China. The highly suitable area (with suitability between 66 and 100) was mainly concentrated in Northeast Sichuan, South Shaanxi, most of Chongqing, West Hubei and Southwest Gansu and occupied 4.94% of land in China. Under different future emission scenarios, both the areas and the centers of the suitable areas all showed differences compared with the current situation. Four climatic variables, i.e., maximum April temperature (19%), mean temperature of the coldest quarter (14%), precipitation in May (11.5%) and minimum temperature in October (10.8%), had the largest impact on the distribution of Psa.

Conclusion

The MaxEnt model is potentially useful for forecasting the future adaptive distribution of Psa under climate change, and it provides important guidance for comprehensive management.

Introduction

Kiwifruit, Actinidiaceae, *Actinidia* Lindl., is a type of perennial, deciduous woody liana and an important class of berry fruit. There are sixty-six different species in the Actinidiaceae family, sixty-two of which originated in China [1, 2]. "Hayward" is the most popular variety of kiwifruit grown across the world, and it was selected in New Zealand from seeds coming from Yichang City, Hubei Province in 1904. As a rich nutritional source of sugar, protein, amino acids and vitamins, and an especially high vitamin C content, the kiwifruit is known as "the king of the fruit" and has good market prospects. The main areas of kiwifruit production in China are in the northern foot of the Qinling Mountains in Shaanxi Province, the Dabie Mountain area in Anhui Province, Heping County in Guangdong Province, Guizhou Plateau, western part of Hunan Province, and Northwest Sichuan Province. Worldwide, kiwifruit is economically very important, and production reached 3.26 million tonnes per year as of 2013. China is the largest kiwifruit producer, with more than 1.77 million tonnes per year, placing China ahead of Italy. The kiwifruit industry, which developed quickly in recent years, has become one of the specialty industries in China that promotes agricultural development [3, 4].

Bacterial canker of kiwifruit caused by *Pseudomonas syringae pv. actinidiae* (Psa) is a destructive disease of kiwifruit that causes great losses in kiwifruit production. The disease not only causes great economic losses but also increases the plant mortality of kiwifruit, and to date, there has not been an effective control measure identified [5, 6]. The symptoms and the infection cycle of bacterial canker are consistent throughout the world [7–9]. Symptoms usually appear in the spring or autumn under climatic conditions that are suitable for disease development. The canker spots can occur on twigs, trunks, leaves and flowers. It first appears as a watery lesion on twigs and trunks, then expands into a white exudation, and eventually turns into a rusty-red profuse exudation [10]. Affected branches necrose, water and nutrient transport are restricted, eventually causing the plant organs to wither and die. The symptoms on the leaves began to appear in early April, when the chlorosis transitions from pale brown to tan; it eventually becomes dark-brown with a surrounding yellow halo and finally wilts and curls. When the buds are infected, the growth rate slows or even prevents flowering, which results in fruit drop or the formation of deformed fruit [11].

In 1984, Psa was first isolated from 'Hayward' (a type of *Actinidia deliciosa* with green flesh) in Japan [12]. Currently, the pathogen is widely distributed in the major producing countries of kiwifruit, including China, New Zealand, Italy, South Korea, Iran, France, Portugal, Chile, Spain, Switzerland and Australia, as well as in other countries [13, 14]. In China, the kiwifruit bacterial canker was first discovered in the Dongshan Peak farm of Hunan Province in 1985 [15]. The disease quickly spread to the provinces of Sichuan, Anhui, Hunan and Shaanxi[16]. In Japan and Korea, outbreaks of kiwifruit bacterial canker have mainly affected the 'Hayward' cultivar. However, in China and other countries, the disease was highly destructive on cultivars of both *A. deliciosa* and *A. chinensis*. In Shaanxi Province in 2012, an outbreak of kiwifruit canker was recorded in a red-fleshed cultivar of 'Hongyang' and in a green-fleshed kiwifruit cultivar of 'Xuxiang'. The percentage of trees impacted by the disease ranged from 20% to 70%, even up to 100% in some places [17]. An investigation into the bacterial canker of kiwifruit in

Sichuan Province between 2014 and 2016 showed that the disease had common occurrence patterns in different production areas, and the situation is worsening as growing areas expand.

Presently, due to the economic losses and the great destruction to the industry, kiwifruit bacterial canker is considered as the major threat for the cultivation of kiwifruit around the world. As a highly infectious disease, its pathogen (*Pseudomonas syringae pv. actinidiae*) has been listed on the A2 List of the Mediterranean Plant Protection Organization (EPPO) [18]. In 1996, the State Forestry Administration of China included Psa on the quarantine list of nation-wide objects of forest plants. In 2009, China's General Administration of Quality Supervision issued a new document on the relevant requirements for prohibiting the entry of Psa into China [19].

The study of suitable habitat is an important field of ecology, and the species distribution model (SDM) has evolved and become an important tool for studying the suitability of a habitat for a particular species [20]. The SDM assumes a species niche should be conserved over space and time, assesses the potential geographical distribution of a target species based on presence/absence data and uses the corresponding mathematical variables to determine habitat preferences for a species. At present, SDMs are mainly applied and influence the following aspects: research on species' potential geographical distribution, analysis of the relationship between species distribution and climate change, prediction of the habitat suitability of endangered species, and the study of paleogeography [21]. An SDM model, i.e., the maximum entropy model (MaxEnt), has many advantages, including short running time, easy operation, small sample size and high simulation precision, and was applied to simulate the suitable geographical distribution of species suitability [22–24]. In recent years, many researchers have used MaxEnt to simulate the distribution of many plant diseases, such as citrus huanglongbing (caused by *Candidatus liberibacter*) [25], maize downy mildew (caused by *Peronosclerospora maydis*) [26], wheat blast (caused by *Magnaporhe grisea*) [27], South American leaf blight (caused by *Microcyclus ulei*) [28], and pine wilt disease (caused by *Bursaphelenchus xylophilus*) [29]. MaxEnt performs well in this type of application and is widely accepted by ecologists.

Climate change has greatly influenced the distribution of various species, and future climate change will change the habitat, range, and distribution of many species [30–32]. Plant disease is one of the most serious biological disasters to impact agricultural production and is constrained by climate change, host plants, tillage management and farming systems [33–35]. The distribution and abundance of plant diseases are highly influenced by climatic factors (i.e., temperature, moisture, humidity and their seasonal variations) [36, 37]. Temperature is one of the most influential environmental factors affecting the distribution and abundance of different species [38, 39]. In the context of global climate change, where trends indicate increasing temperatures, variations in precipitation and more frequent and extreme weather events have occurred. Additionally, the environment has changed, which has resulted in changes in the areas and periods of plant diseases and led to changes in distribution, occurrence, epidemiology and population structure [40, 41]. SDM is an effective tool for studying the impact of future climate change on species distribution and provides a variety of realistic scenarios to expound the influence of climatic factors on the epidemiological traits of pathogens. SDMs utilize a series of greenhouse gas emission scenarios, which are based on global climate models (GCMs), to analyze the influence of climate change on current and future habitat suitability of various species [42]. Accurate predictions regarding the future state of species will not be provided in SDM at any given point in time, but the possible niche that species may occupy in the future is provided [43].

Present studies of Psa are mainly focused on species classification [7, 44], molecular biology [45–47], analysis of biological characteristics [48, 49], pathogenicity differentiation[50–52], rapid detection methods [48, 53, 54], and disease control [55, 56]; however, systemic research

about the influence of climate change on the niches specific to Psa is lacking. In an effort to analyze the effects of climate change on the potential distribution of Psa, MaxEnt was utilized to model the current niches of Psa in China, as well as the future Psa niches under climate change scenarios; additionally, this study identified climatic variables important for the potential establishment of Psa. These results can provide an important reference and theoretical basis for the development of reasonable prevention and control measures.

Materials and methods

Occurrence records of Psa

In this study, the occurrence points of Psa were obtained from field data collected by the authors in the Chinese provinces of Sichuan and Shaanxi, from the published literature, and from the online databases GBIF and EPPO (S1 Table). When coordinates were published, we used the records directly. If there were only localities, Google Earth was used to collect coordinates of the records. All occurrence records were checked for accuracy in ArcGIS prior to use. Records with obvious geocoding errors were discarded, and duplicate records were removed manually. All records were imported into Microsoft Excel and saved as "*.CSV" format.

Environmental variables

From the WorldClim database (http://www.worldclim.org), we obtained 67 environmental variables (19 bioclimatic variables and 48 monthly averages of temperature and precipitation) for the current period [57, 58]. In the Worldclim database, 'current period' was defined from 1950 to 2000, and these data have been widely used in creating species distribution models. In 2013, the Fifth Assessment Report was released by the UN's Intergovernmental Panel on Climate Change (IPCC), and four representative concentration pathways (RCPs, including RCP2.6, RCP4.5, RCP6.0 and RCP8.5) were published in the report [59, 60]. The impacts of climate change strategies on greenhouse gas emissions are considered more in the RCPs scenarios, and the projection of future climate change is more scientifically described. RCP4.5 and RCP6.0 are medium greenhouse gas emission scenarios, and RCP4.5 is of higher priority than RCP6.0 [61, 62]. Therefore, RCP2.6 (the minimum greenhouse gas emission scenario), RCP4.5 (the medium greenhouse gas emission scenario) and RCP8.5 (the maximum greenhouse gas emission scenario) for the 2030s (2021–2040), 2050s (2041–2060), 2070s (2061–2080) and 2080s (2071–2090) were selected for the future model prediction of Psa in China. The future environmental variables were downloaded from the Climate Change, Agriculture and Food Security (CCAFS) website. All environmental variables were in raster format with a 2.5-arc minute resolution (~4.5 km^2).

Environmental variables derived from WorldClim and CCAFS, which has been widely used in the prediction of the potential distribution of species, can reflect the characteristics of temperature and precipitation as well as their seasonal variation characteristics. The 19 bioclimatic variables with strong biological significance explained the adaptation of species with extreme environmental factors. These variables were also suitable for describing the distribution of species across large scales such as the intercontinental scale [63, 64]. Due to the various reasons mentioned above, the environmental variables provided above were chosen as the initial variables to be used in the modeling in this article. Based on Worthington's [65] method on how to filter available variables for modeling, the jackknife test was used to evaluate each variable's contribution to the simulation, and 25 variables were removed due to their lack of contribution (percent contribution = 0). Next, the highly correlated variables were eliminated, and variables with a Pearson's $|r| \leq 0.8$ were retained. After this process, 22 variables (S2 Table) were retained to simulate the current and future distributions of Psa in China.

Distribution modeling

MaxEnt software was utilized to predict the suitable habitat distribution of Psa in China [66]. MaxEnt uses presence-only and small sample size data to model habitat suitability as a function of environmental variables, and it is consistently among the highest performing SDM methods [67]. Response curves indicate the relationships between climatic variables, and the predicted probability of the presence of Psa was determined by MaxEnt. The percent contribution and permutation importance of environmental variables were calculated, and jackknife procedures were executed in MaxEnt. These analysis methods are all useful to measure the importance of the environmental variables. There were 10 replicates, and a random test percentage was chosen for each replicate. The remaining model values were set to default values [68–71].

MaxEnt estimates the probability a species will be present based on presence records and randomly generates background points by finding the maximum entropy distribution. An estimate of habitat suitability for a species was exported from MaxEnt, and its range generally varied from 0 (lowest) to 1 (highest). Model predictions were imported into a geographic information system (GIS), and maps were generated using ArcMap. Four arbitrary categories of habitat suitability for Psa were defined as no suitability (0–5), low suitability (5–33), medium suitability (33–66) and high suitability (66–100) based on predicted habitat suitability.

In this study, the ROC curve method was utilized to assess the model's explanatory power [72]. The AUC (area under roc curve) is an effective threshold-independent index that can evaluate a model's ability to discriminate presence from absence (or background). The evaluation criterion of AUC is illustrated in S3 Table [63].

For reducing the bias of estimation, in 1949, Quenouille [73] proposed an unbiased method of nonparametric estimation, and Tukey renamed it jackknife in 1958 [74]. This method can estimate parameters and adjust the deviation without assumptions of distribution probability. In SDM, the jackknife method was used to analyze the effects of environmental variables on model results to choose dominant factors. The specific process involves 1. Calculating the training gain for the model with only variable. Higher training gain indicates that the variable has high prediction power and contributes greatly to species distribution; 2. Calculating the training gain for the model without a specific variable and analyzing the correlation between the removed variable and the omission error. If the removal of an environmental variable leads to a significant increase in the omission error, it indicates that the variable has a significant effect on the model's prediction; 3. Calculating the training gain for the model with all variables [68].

Models of the mean center of highly suitable areas

The mean centers of highly suitable areas of Psa in China were calculated according to Yue's [75] formula:

$$
\begin{cases}
x(t) = \sum_{i=1}^{I} \dfrac{s_i(t) \bullet X_i(t)}{S(t)} \\[2ex]
y(t) = \sum_{i=1}^{I} \dfrac{s_i(t) \bullet Y_i(t)}{S(t)}
\end{cases}
$$

In this formula, *t* is the variable of time (i.e., current, 2030s, 2050s, 2070s and 2080s), *I* is the patch number of highly suitable areas, *Si(t)* is the area of *i*th patch of highly suitable areas, *S(t)* is the total area of highly suitable areas, (*Xi(t)*, *Yi(t)*) are the longitudinal and latitudinal

coordinate, respectively, of the geometric center of the *i*th patch of highly suitable areas, and (*x* (*t*), *y(t)*) are the mean centers of the highly suitable areas. The shift in distance and direction of highly suitable areas in the period from *t* to *t* + 1 are, respectively, formulated as Yue [75],

$$D = \sqrt{(x(t+1) - x(t))^2 + (y(t+1) - y(t))^2}$$

$$\theta = \text{arctg}\left(\frac{y(t+1) - y(t)}{x(t+1) - x(t)}\right)$$

where *D* is the shift in distance of the highly suitable area during the period of *t* to *t*+1; *θ* is the shift in direction of the highly suitable areas, where east is defined as 0˚, north is defined as 90˚, west is defined as 180˚ and south is defined as 270˚.

Describe the same contents as "Materials and methods" sections with step-by-step protocol on my protocols.io: http://dx.doi.org/10.17504/protocols.io.mdic24e

Results

Model performance and contributions of variables

In this study, from the ROC curves, AUC values were used to evaluate the performance of the MaxEnt model. Many studies showed that an AUC of high values led to better results that significantly differed from the random predictions. The accuracy of prediction of Psa during the current period was found to be "excellent" (AUC_{mean} = 0.963, Fig 1) according to the identified evaluation criteria (S3 Table).

Fig 2 shows that the MaxEnt models that predicted the distribution of Psa in the future period performed "excellent", with high AUC values (0.949–0.964). The results indicate that the simulations have high reliability and can be used to analyze the impact of climate change on the distribution of Psa in China.

Among the environmental variables, the maximum temperature in April (19%), mean temperature of coldest quarter (14%), precipitation in May (11.5%) and minimum temperature in October (10.8%) played major roles in the spread of Psa (Table 1 and Fig 3) and individually contributed more to run the model. The other 18 environmental variables, including temperature (maximum temperature in September, October, November, and December; minimum temperature in March, April, and November; mean temperature in May; mean diurnal range, max temperature of the warmest month, min temperature of the coldest month, annual temperature range, mean temperature of the driest quarter), annual precipitation (precipitation in September and December, annual precipitation, precipitation of the driest month) and altitude, individually contributed less (a combined total contribution of 44.7%) to run the model. Considering the importance of permutation, the mean temperature in May (21.8%), mean temperature of coldest quarter (14.8%) and mean diurnal range (10%) each played a vital role in predicting the probable distribution of Psa, and individually, they contributed more than the other variables to run the model.

Predicting the distribution of Psa in China

ArcGIS 10.0 was used to analyze the simulation results from the MaxEnt model for further study. The result showed that the area from latitude 25˚ to 36˚N and from longitude 101˚ to 122˚E was the primary potential suitable region of Psa in China. Based on the division criteria of suitability for Psa, the main suitable regions of Psa in China were extracted by ArcGIS (Fig 4). The potential suitable areas were mainly located in the provinces of Sichuan, Shaanxi, Chongqing, Hubei, Zhejiang, Gansu, Guizhou, Hunan, Jiangsu, Henan and Anhui, which
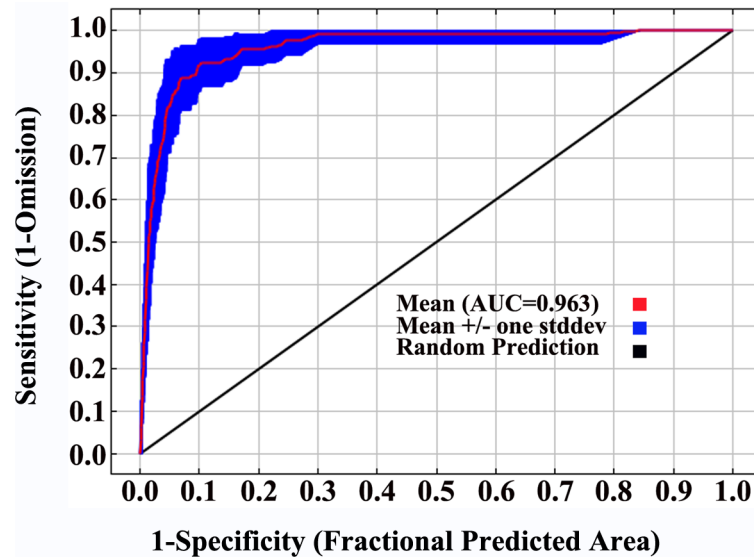
Fig 1. ROC curve and AUC value under the current period (10 runs). The current period is from 1950 to 2000.

occupied 27.78% of the land of China. The highly suitable area (with suitability values between 66 and 100) was mainly concentrated in Northeast Sichuan, South Shaanxi, most of Chongqing, West Hubei and Southwest Gansu. The areas of highly suitable areas in the major producing provinces were analyzed statistically (Table 2), and it showed that the most suitable areas of Psa occupied 4.94% of the land of China. Sichuan (1.38%), Shaanxi (0.84%), Hubei (0.6%), Chongqing (0.59%) and Zhejiang (0.48%) were considered to be the major suitable provinces for Psa.

Area change, shift in distance and direction of mean centers of Psa under climate change scenarios

Under scenario RCP2.6 (Table 3 and Fig 5), comparing the future suitable areas with the current suitable areas showed that areas of high suitability would have the greatest increase in the 2080s; the increase would be 11.71×10^4 km^2 and account for 124.63% of the current predicted area. From the present to the 2080s, the mean centers of highly suitable areas would shift from Yunyang (current) to Jianshi (2030s), Fengjie (2050s and 2070s) and Enshi (2080s). The shift in distance of the mean centers from the present location to the simulated location in the 2080s is approximately 73.87 km to the southeast (Table 4 and Fig 6).

Scenario RCP4.5 indicated that the highly suitable areas would increase 7.02×10^4 km^2, 4.73×10^4 km^2, 2.41×10^4 km^2, 3.48×10^4 km^2, respectively (Table 3 and Fig 5). The mean centers would shift from Yunyang (current) to Fengjie (2030s), Enshi (2050s), Fengjie (2070s) and Yunyang (2080s). The shift in distance of the mean centers from the present location to the simulated location in the 2080s is approximately 44.31 km to the northeast (Table 4 and Fig 6).

Under scenario RCP8.5 (Table 3 and Fig 5), the highly suitable areas showed a decreasing trend from the present to the 2080s, and the reductions would be 0.04×10^4 km^2, 1.18×10^4 km^2, 9.66×10^4 km^2 and 3.45×10^4 km^2, respectively. The mean centers of highly suitable areas would shift from Yunyang (Current) to Shengnongjia (2030s), Wuxi (2050s), Kaizhou (2070s) and Wuxi (2080s). The shift in distance of the mean centers from the present to the 2080s is approximately 50.83 km to the northeast (Table 4 and Fig 6).
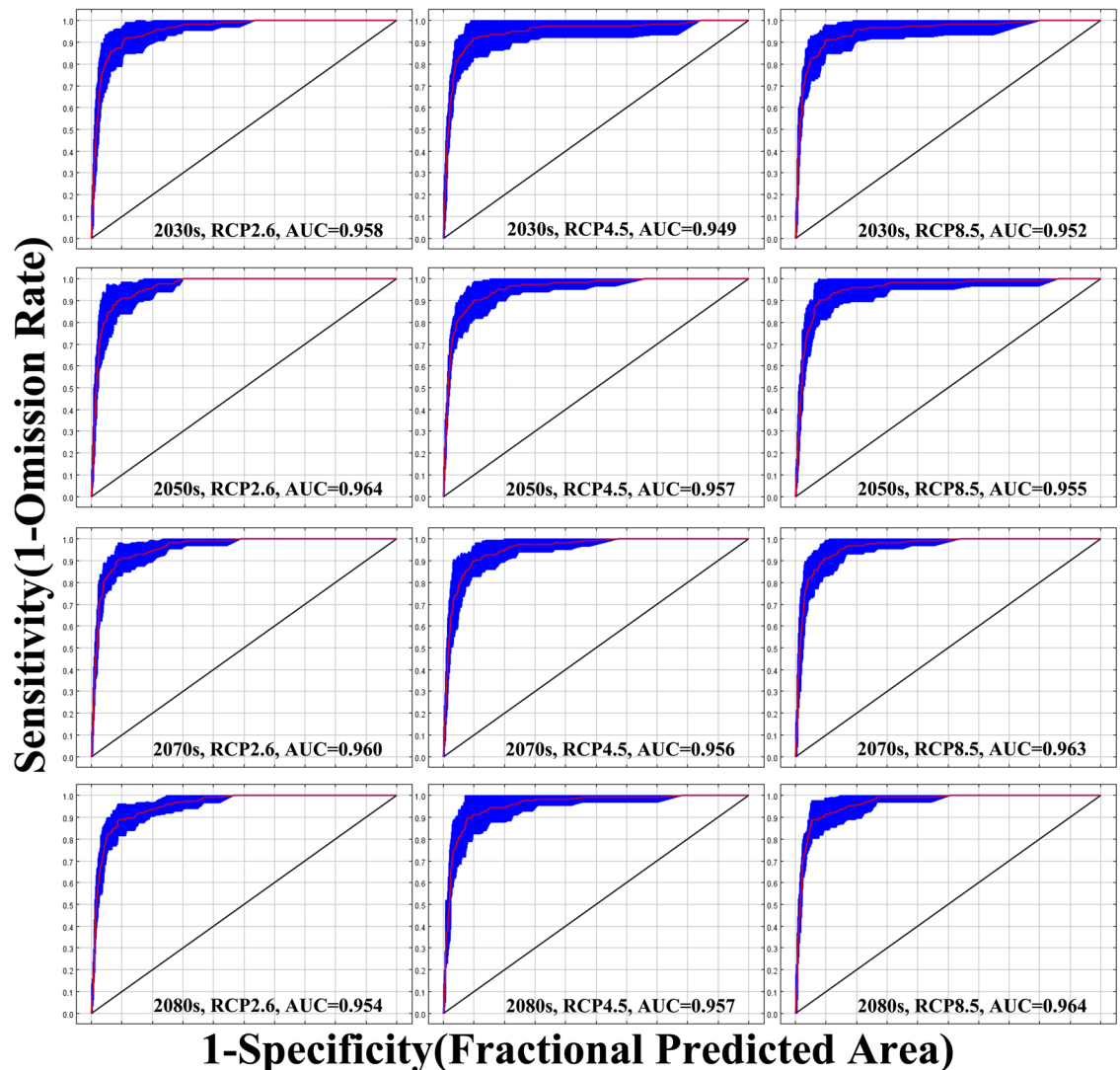
Fig 2. ROC curves and AUC values in future periods. The future periods is 2030s (2021–2040), 2050s (2041–2060), 2070s (2061–2080) and 2080s (2071–2090).

https://doi.org/10.1371/journal.pone.0192153.g002

Response of variables to suitability

Response curves indicated the relationships between environmental variables and the predicted probability of the presence of Psa. Individual response curves for different variables (model created using only the corresponding variable) showed that the predicted probability of the presence of Psa showed a similar pattern to the Poisson distribution (Table 5 and Fig 7).

According to the response curve of mean temperature of the coldest quarter, the probability of Psa occurrence increased up to 8.1˚C and deceased sharply after that. Similar trends were observed for maximum temperature in April, and the response curve indicated that Psa would survive in locations where the maximum temperature in April was between 13.7–23.6˚C; however, the probability of Psa decreased rapidly above 21.2˚C. The response curve of precipitation in May indicated that higher levels of precipitation (50.1–317 mm) in May would be conducive for the development of cankers caused by Psa. The response curve of the minimum

Table 1. Estimates of contribution and permutation importance of environmental variables in MaxEnt modeling of Psa.

Variables	Percent contribution	Permutation importance
Maximum temperature in April (˚C)	19	2.3
Mean temperature of the coldest quarter (˚C)	14	14.8
Precipitation in May (mm)	11.5	2.6
Minimum temperature in October (˚C)	10.8	1
Maximum temperature in October (˚C)	8.7	0.5
Precipitation in September (mm)	6.4	5.4
Mean diurnal range (˚C)	5.7	10
Minimum temperature of the coldest month (˚C)	3.8	7.7
Maximum temperature in February (˚C)	2.9	0.2
Annual temperature range (˚C)	2.7	5
Maximum temperature in December (˚C)	2.6	1.1
Annual precipitation (mm)	2.3	2.7
Maximum temperature in September (˚C)	1.7	0.4
Altitude (m)	1.3	2.2
Maximum temperature of the warmest month (˚C)	1.2	2.7
Mean temperature of the driest quarter (˚C)	1.1	7.5
Mean temperature in May (˚C)	1.1	21.8
Minimum temperature in November (˚C)	0.8	0.6
Minimum temperature in April (˚C)	0.7	0.3
Precipitation of the driest month (mm)	0.6	1.7
Precipitation in December (mm)	0.6	7.4
Minimum temperature in March (˚C)	0.4	1.7
Maximum temperature in November (˚C)	0.1	0.1

temperature in October showed that Psa can tolerate a wider range of temperatures (3.6 to 17.1˚C) in October.

Discussion

Model selection and evaluation

At present, most studies researching Psa are concentrated on small-scale ranges, while there are relatively few studies that examine the potential geographic distribution of Psa on large scales and model future niches under climate change scenarios. Based on the maximum entropy principle, the MaxEnt software uses the species distribution data and the environmental variables to analyze the distribution state of the species when the entropy is the largest [76]. Numerous studies show that MaxEnt performs better than other niche models and has advantages, such as short running time, easy operation, small sample size and high simulation precision [68, 77–79]; therefore, this study was designed to examine the large scale and future distribution of Psa using MaxEnt theory.

The results showed that the choice of environmental variables has a certain influence on the prediction results of niche models. Many researchers that use the MaxEnt model to predict the geographical distribution of species non-selectively use all of the environmental factors or the major environmental factors [59, 80–82]. The environmental variables, which were obtained from the WorldClim database and CCAFS, are based on temperature and rainfall data based on the different needs of the occurrence calculations. Therefore, there are inevitable relationships between the auto correlation of these variables, multiple linear repetition and other
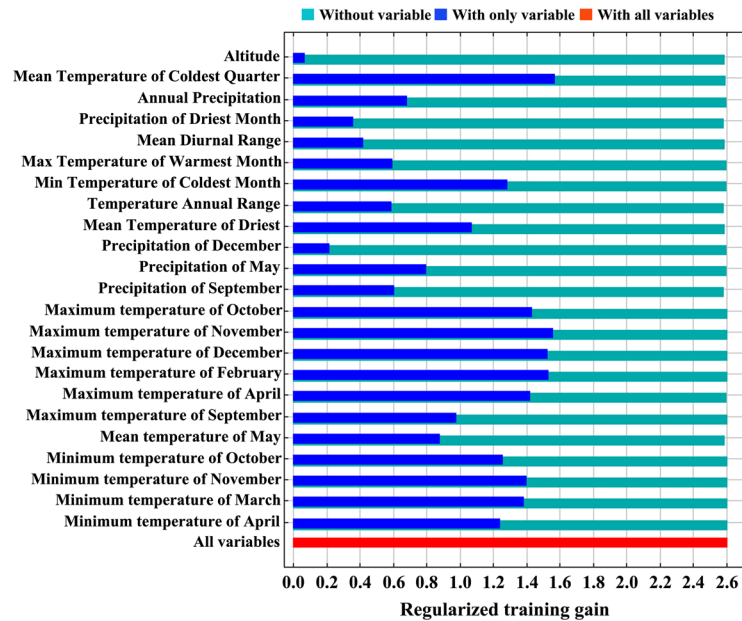
Fig 3. Jackknife test for variable importance of Psa habitat suitability distribution. Values shown are averages over 10 replicate runs.

issues. Studies have confirmed that these highly relevant variables introduce redundant information into the model prediction process, which affects the prediction results [65, 83, 84]. To avoid these problems when modeling, relevant analysis and effective screening of environmental variables should be carried out before subsequent analyses occurs. In this study, the importance of the variables was evaluated by examining the contribution rate of each factor to species distribution. The environmental variables with small contribution rates were excluded, and the correlation of the selected variables was analyzed using only the leading the environmental variables; additionally, the model was reconstructed to reduce the impact of redundant information on the simulation results and to improve the accuracy of the prediction results.

At present, the most widely used method for model accuracy evaluation is the ROC curve method (AUC method). Because AUC is not affected by diagnostic thresholds, as it provides performance evaluation results at all threshold ranges, it is now recognized as a niche model evaluator. AUC values range from 0.5 to 1, where the closer the value is to 1, the higher the accuracy of the model [85, 86]. In this study, the AUC average values of the simulated training set based on the dominant environmental variables were greater than 0.949 (i.e., very close to 1), and the predicted results reached the "excellent" level, indicating that the geographical distribution of the predicted model is in high agreement with the actual distribution. In addition, this study used ArcGIS to postulate the raster files of the MaxEnt output so that the distribution data of the target species and the environmental variable data corresponded to the grid cells, effectively reduced system error, and further improved the accuracy of the data.

Predicting the distribution of Psa in China

The present use of GIS technology to simulate the spatial distribution patterns of species is an important tool. More and more studies have used GIS and statistical analysis methods to identify the relationship between species richness and spatial heterogeneity [87–89]. In this study, a combination of MaxEnt and ArcGIS was used to predict the potential geographic distribution
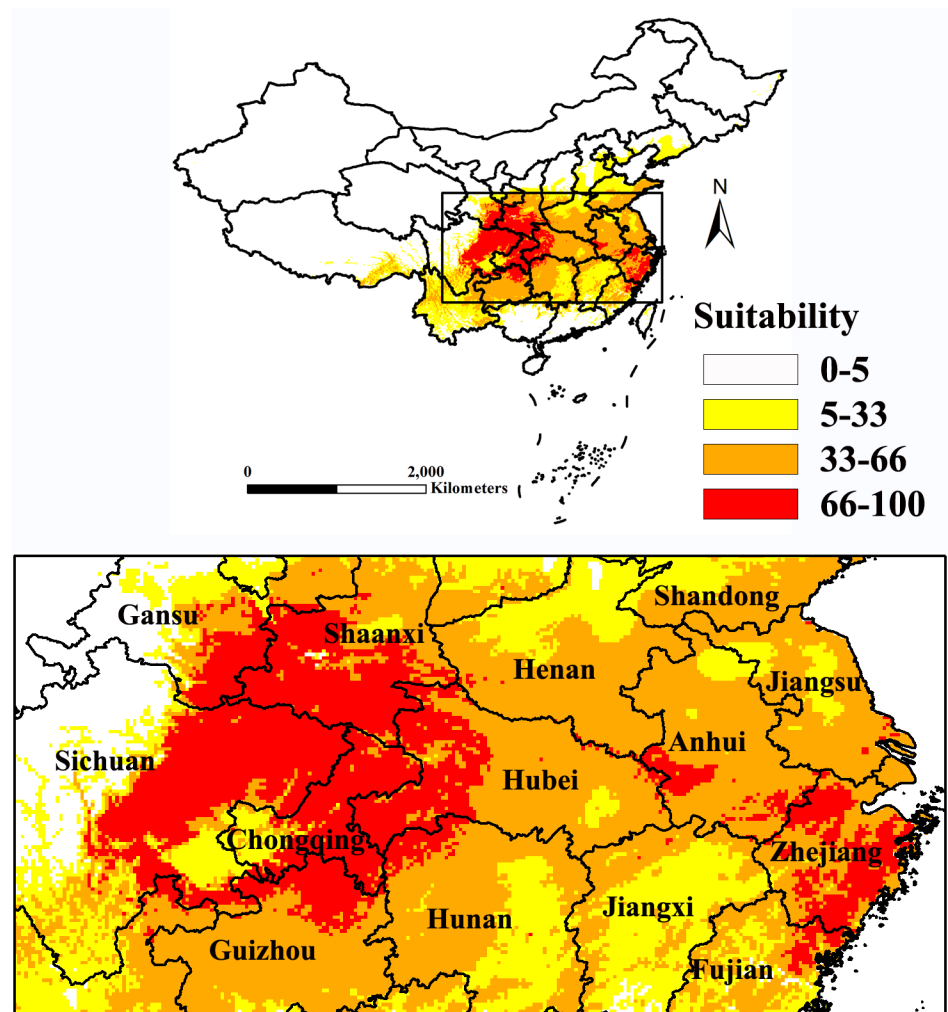
Fig 4. Distribution of core suitable areas of Psa under current climate condition in China. The probability of Psa is shown in the color scale in the legend. Red indicates highly suitable area with >66 probability of occurrence, orange indicates moderately suitable area with 33–66 probability of occurrence, yellow indicates poorly suitable area with 5–33 probability of occurrence and white indicates unsuitable area.

https://doi.org/10.1371/journal.pone.0192153.g004

Table 2. Analysis of highly suitable main distributions of Psa.

Province	Highly suitable (km²)	Total (km²)	Percentage (of highly suitable areas in the province, %)	Percentage (of highly suitable areas in China, %)
Sichuan	133055.6	455139	29.23	1.38
Shaanxi	81111.11	204167	39.73	0.84
Chongqing	56319.44	77083	73.06	0.59
Hubei	57569.44	175556	32.79	0.60
Zhejiang	46111.11	94816	48.63	0.48
Gansu	29166.67	414930	7.03	0.30
Guizhou	28680.56	159722	17.96	0.30
Anhui	16319.44	133680	12.21	0.17
Hunan	12083.33	194374	6.22	0.13
Henan	2013.89	161180	1.25	0.02
China	475486.11	9618680	—	4.94

https://doi.org/10.1371/journal.pone.0192153.t002

**Table 3. Predicted suitable areas for Psa under current and future climatic conditions.**

Decade	Scenarios	Predicted area/×10^4 km^2			Account of the proportion of current predicted area (%)		
		Poorly	**Moderately**	**Highly**	**Poorly**	**Moderately**	**Highly**
Current	—	102.17	118.13	47.55	—	—	—
2030s	RCP2.6	102	119.41	56.89	99.83	101.09	119.64
	RCP4.5	114.64	115.55	54.57	112.2	97.81	114.77
	RCP8.5	111.22	118.01	47.51	108.85	99.89	99.92
2050s	RCP2.6	114.74	124.18	48.41	112.3	105.11	101.81
	RCP4.5	106.69	111.06	52.28	104.42	94.01	109.96
	RCP8.5	123.56	117.95	46.37	120.94	99.84	97.52
2070s	RCP2.6	120.95	130.33	47.95	118.38	110.32	100.85
	RCP4.5	115.83	126.8	49.96	113.37	107.34	105.06
	RCP8.5	129.68	131.97	37.89	126.92	111.72	79.71
2080s	RCP2.6	112.06	119.01	59.26	109.68	100.71	124.63
	RCP4.5	104.47	124.57	51.03	102.24	105.54	107.32
	RCP8.5	166.13	123.47	44.1	162.6	104.52	92.74

of Psa in China. The results showed that, under current climatic conditions, the area from latitude 25˚ to 36˚N and from longitude 101˚ to 122˚E is the primary potential suitable area of Psa in China. The highly suitable area was mainly concentrated in Northeast Sichuan, South Shaanxi, most of Chongqing, West Hubei and Southwest Gansu and occupied 4.94% of land in China. From 2014 to 2016, we investigated the occurrence of kiwifruit bacterial canker in Sichuan and Shaanxi provinces. The result showed that the disease is mainly distributed in Guangyuan, Bazhong, Mianyang, Chengdu, Yaan and Yibin in Sichuan province, and in Xian, Baoji and Weinan in Shaanxi province. The potential distribution of this study was highly coincident with the locations of field surveys in Shaanxi and Sichuan. In an earlier study, Shao et al [19] simulated the potential distribution of Psa at the state level using a fuzzy mathematics comprehensive evaluation. The results showed that potential areas of the pathogen were mainly distributed in Sichuan, Yunnan, Guizho, Fujian, Anhui, Hunan, Hubei, Henan, Jiangxi, Shaanxi, Zhejiang, Chongqing and Tibet. Our model predictions are aligned with the predictions of Shao et al [19].in most of the kiwifruit growing areas, but they significantly differed in other areas such as Yunnan and Tibet. The differences could be due to the model simulation theory and specific assumptions, types of environmental variables and calibration settings. For instance, as a type of correlative model, fuzzy mathematics comprehensive evaluation based on direct measures of physiological variables ignores biotic interactions, while MaxEnt is based on observations and includes the effects of biotic interactions.

In this study, the area under three climate change scenarios was statistically analyzed with ArcGIS to identify the trends of the area impacted by disease. The results showed that under both scenario RCP2.6 and scenario RCP4.5, suitable areas of Psa would increase until the 2080s; in contrast, under scenario RCP8.5, the highly suitable areas decreased from the present until the 2080s. This indicated that different emission scenarios have different and opposite effects on the potential distribution of Psa in China.

Climate is a decisive factor in species distribution, while changes in species distribution patterns are the most clear and direct reflection of climate change. Climate change characteristics influenced by global warming have been changing the structure and function of terrestrial ecosystems, thus changing the biological habitats and geographical distribution of species [32, 36, 38, 41]. To understand the response of Psa to climate change, we calculated and analyzed the position of the mean center in different grades and the center's shift over time based on the
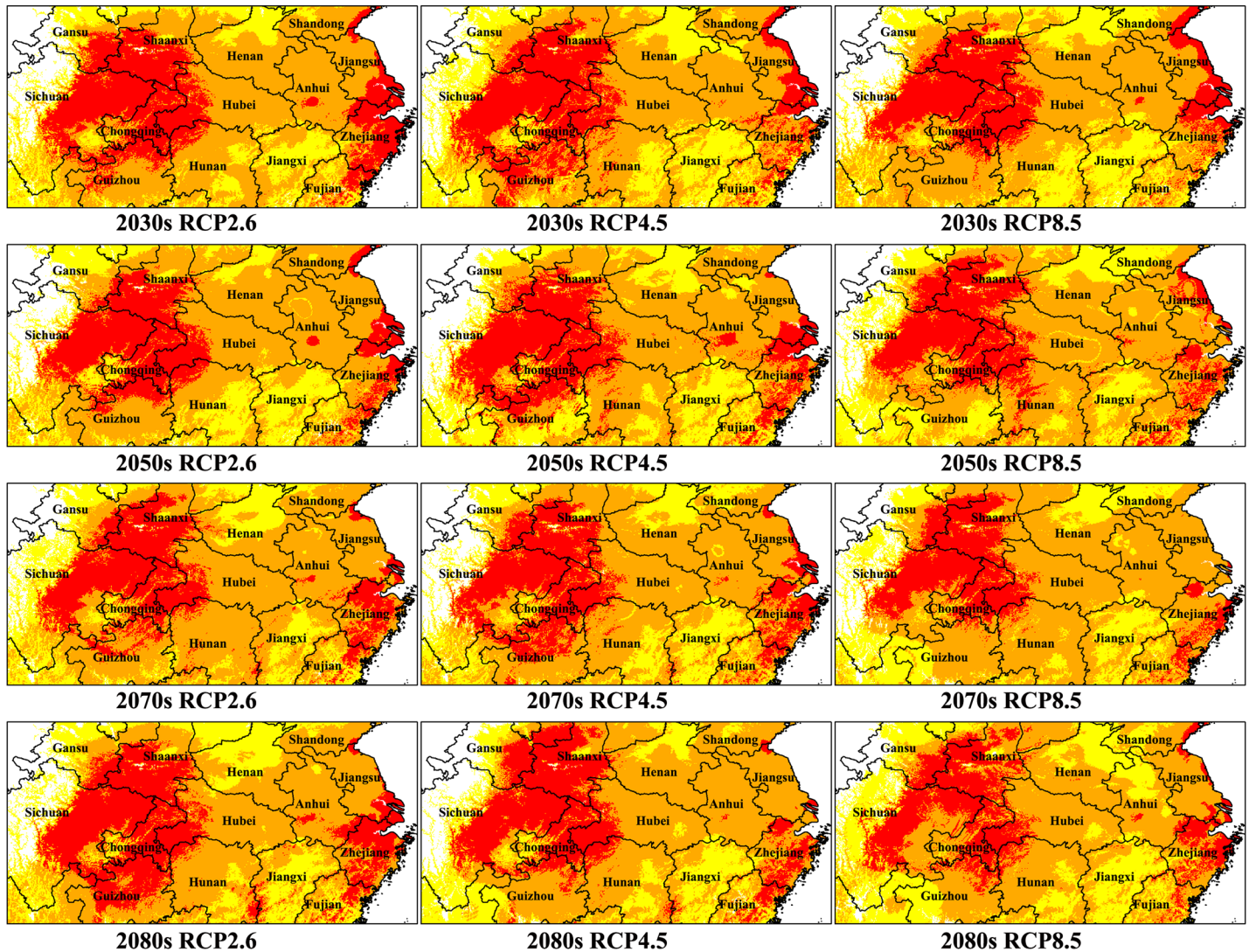
Fig 5. Distribution of core suitable areas of Psa under different climate change scenarios in China. The probability of Psa is shown in the color scale in the legend. Red indicates highly suitable area with >66 probability of occurrence, orange indicates moderately suitable area with 33–66 probability of occurrence, yellow indicates poorly suitable area with 5–33 probability of occurrence and white indicates unsuitable area of occurrence.

calculation method used by Yue et al [75]. The results showed that mean centers of highly suitable areas will change in a variety of ways under the three emission scenarios until the 2080s. Under scenario RCP4.5 and scenario RCP8.5, the mean centers will move to the northwest. The movement may be related to the increase in the average temperature and precipitation. In addition, from the simulation results, no obvious regularities were found in the location and displacement of the mean centers under the different scenarios. This may be due to the lack of continuity between current and future climate variables. The current period is from 1950 to 2000, while the future period is from 2030 to 2080, and there is a gap between 2000 and 2030.

Table 4. Shifts in distance and direction of the mean centers of highly suitable areas in different periods.

Period	RCP2.6		RCP4.5		RCP8.5	
	Displacement (km)	Direction	Displacement (km)	Direction	Displacement(km)	Direction
From T1 to T2	98.89	Southeast	5.84	Southeast	111	Northeast
From T2 to T3	58.22	Northwest	38.38	Southeast	61.26	Southwest
From T3 to T4	13.24	Northeast	31.05	Northeast	100.83	Northwest
From T4 to T5	61.53	Southeast	83.58	Northwest	98.31	Southeast
From T1 to T5	73.87	Southeast	44.31	Northwest	50.83	Northeast

The reciprocating movement of the mean center may be due to the lack of data during this period.

Effects of climatic factors on the distribution of Psa

Studying the interaction between species and the environment is an essential aspect of species ecology[90]. The relationship between the probability of species presence and dominant
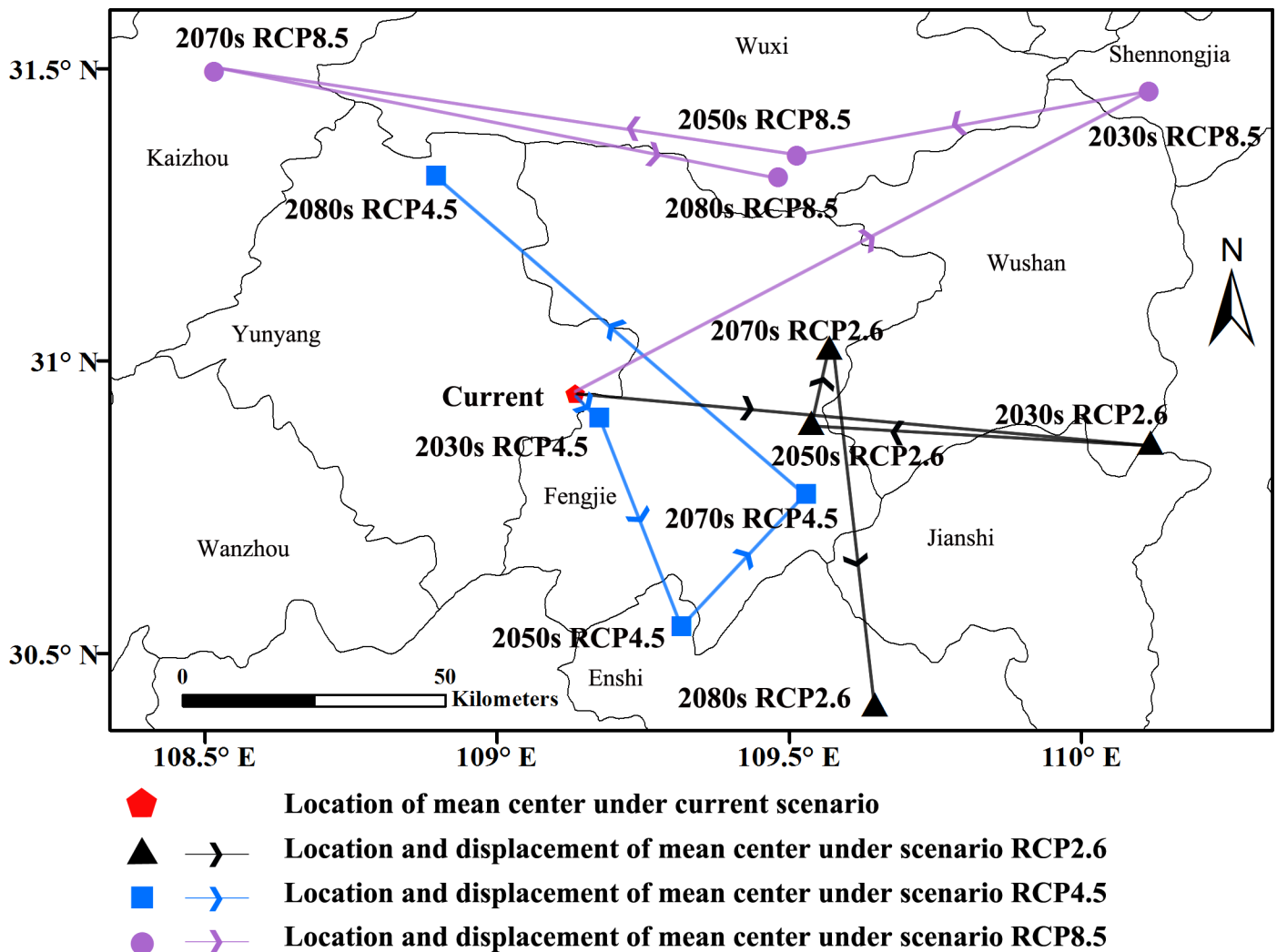

Fig 6. Center displacement of highly suitable areas during different periods.

Table 5. The suitable range of dominant environmental variables affecting the potential distribution of Psa.

Environmental variables	Suitable range	Optimum value
Maximum temperature in April (˚C)	13.7–23.6	21.2
Mean Temperature of the Coldest Quarter (˚C)	-3.9–9.3	8.1
Precipitation in May (mm)	50.1–317	83
Minimum temperature in October (˚C)	3.6–17.1	10.3

environmental variables was analyzed in this paper, and the response curves were created by MaxEnt. The analysis showed that the probability of species presence changed as a result of the dominant environmental variables (maximum temperature in April, mean temperature of the coldest quarter, precipitation in May and minimum temperature in October). Both the precipitation and temperature variables were strongly correlated with the distribution of Psa. Our results were in good agreement with some previous research conclusions. For example, previous research by Marcelletti and Scortichini found low temperature, abundant rainfall and high humidity were the most favorable conditions for disease development [91], and this is in accordance with the trends we observed in the response curve of precipitation in May. The model results showed that the probability that Psa would be present decreased rapidly above 21.2˚C, which is consistent with the previous experimental findings of Serizawa and Ichikawa, who found that once temperatures exceeded 25˚C, the harm caused by Psa weakened [91]. Other research showed that when the average temperature reached 20˚C, the spread of the disease was inhibited [92]. Overall, these studies suggested that the occurrence of Psa is closely related to climate, and further studies about this will be useful for predicting and forecasting the kiwifruit canker.

Limitations in this research and the future directions

Although the MaxEnt model predicts the advantages of simple operation, small sample demand and high prediction accuracy, there are some limitations that are similar to other niche prediction models.

1. The environmental variables used in the prediction by the MaxEnt model are all climatic variables except for altitude. The 19 bioclimatic variables are the climatic extremes, i.e., the maximum and the minimum of the actual distribution of Psa. The MaxEnt model shows the maximum likelihood of species distribution and cannot be prepared to express species in the main areas of actual distribution. The above forecast results are more focused on understanding and demonstrating the potential geographical distribution of Psa and revealing the climate characteristics suitable for the distribution of species.

2. The basic niche is an ideal niche, which refers to the maximum niche that a species occupies under ideal living conditions without competition by any other species. The theory only needs to consider the influence of abiotic factors. When the prediction of the suitable area is based not only on the demand of the species in the niche but also on the actual living environment, the biological factors (such as the interaction between species, the vegetation type, geomorphological features, the species own diffusion ability and the soil type) will also have a significant impact on the potential distribution of the predicted species. Based on the above reasons, it can be deduced that the model predicts a niche that is larger than the actual niche occupied by Psa. In this regard, the next step, in addition to considering the impact of climate factors, should consider the interaction between species and other biological factors expressed in order to improve the model's predictive effect.
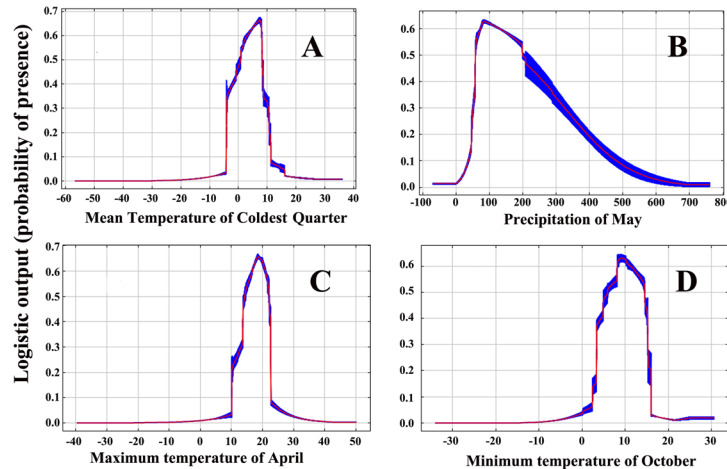
Fig 7. Response curves of the variables contributing most to the prediction by the MaxEnt models for Psa. (A) Mean Temperature of Coldest Quarter (bio11; ˚C). (B) Precipitation of May (prec5; mm), (C) Maximum temperature of April (tmax4; ˚C), (D) Minimum temperature of October (tmin10; ˚C).

3. Over the past 30 years, with the continuous discharge and maintenance of greenhouse gases, the global climate is warming abnormally, and climate change can cause changes in species growth and distribution patterns. The environmental variables used in this study were derived from the world climate database, the WorldClim, which includes data from 1950-2000s; however, this database is missing recent climate data for at least the past 10 years. In the future, the missing data should be filled in so that the forecast results are more accurate and reliable.

Conclusions

In this study, we successfully modeled the current niches of Psa in China, as well as future niches under three climate change scenarios, which allowed for the identification of climatic variables important for the potential establishment of Psa. This study concludes that under scenario RCP2.6 and RCP4.5, the habitat suitability of Psa will increase until the 2080s. We suggest that future climate scenarios should be included in the control measures of Psa, which were created by the institutions responsible for agricultural management.

Supporting information

S1 Table. List of locations used for this study, with longtitude, latitude and sources.
(DOCX)

S2 Table. List of environmental variables used for this study, with type and measurement unit.
(DOCX)

S3 Table. The evaluation criterion of AUC.
(DOCX)

Author Contributions

Conceptualization: Rulin Wang.

Data curation: Rulin Wang, Shisong He, Yuan Liu.

Formal analysis: Rulin Wang.

Funding acquisition: Qing Li.

Investigation: Rulin Wang, Yuan Liu.

Methodology: Rulin Wang, Qing Li.

Project administration: Qing Li.

Resources: Rulin Wang.

Software: Rulin Wang, Gan Jiang.

Supervision: Qing Li.

Validation: Rulin Wang.

Visualization: Rulin Wang.

Writing – original draft: Rulin Wang.

Writing – review & editing: Rulin Wang, Mingtian Wang.

References

1. Wang WC, Chen SY, Zhang XZ. Chloroplast Genome Evolution in Actinidiaceae: clpP Loss, Heterogenous Divergence and Phylogenomic Practice. Plos One. 2016; 9: e0162324. https://doi.org/10.1371/journal.pone.0162324 PMID: 27589600

2. Xu XB, Zhang QM. Researches and Utilizations of Germplasm Resource of Kiwifruit in China. Bulletin of botany. 2003; 6: 648–655.

3. Zhang JL, Mo ZH, Huang SN, Guo ZR. Development of Kiwifruit Industry in the World and Analysis of Trade and International Competitiveness in China Entering 21st Century. Chinese Agricultural Science Bulletin. 2014; 23: 48–55.

4. Testolin R, Ferguson AR. Kiwifruit (Actinidia spp.) production and marketing in Italy. New Zealand Journal of Crop and Horticultural Science. 2009; 1: 1–32. https://doi.org/10.1080/01140670909510246

5. Froud KJ, Beresford RM, Cogger N. Risk factors for kiwifruit bacterial canker disease development in 'Hayward' kiwifruit blocks. Australasian Plant Pathology. 2017; 5: 1–11. https://doi.org/10.1007/s13313-017-0504-1

6. Kim GH, Kim KH, Son KI, Choi ED, Lee YS, Jung JS, et al. Outbreak and Spread of Bacterial Canker of Kiwifruit Caused by Pseudomonas syringae pv. actinidiae Biovar 3 in Korea. Plant Pathology Journal. 2016; 6: 545–551. https://doi.org/10.5423/PPJ.OA.05.2016.0122 PMID: 27904461

7. Vanneste JL, Yu J, Cornish DA, Max S, Clark G. Presence of Pseudomonas syringae pv. actinidiae, the causal agent of bacterial canker of kiwifruit, on symptomatic and asymptomatic tissues of kiwifruit. New Zealand Plant Protection. 2011; 4: 241–245.

8. Balestra GM, Varvaro L. Bacterial diseases on kiwifruit orchards in Italy. Acta Horticulturae. 1999; 498: 355–358. https://doi.org/10.17660/ActaHortic.1999.498.43

9. Kim GH, Jung JS, Koh YJ. Occurrence and Epidemics of Bacterial Canker of Kiwifruit in Korea. Plant Pathology Journal. 2017; 4: 351–361. https://doi.org/10.5423/PPJ.RW.01.2017.0021

10. Vanneste JL. The Scientific, Economic, and Social Impacts of the New Zealand Outbreak of Bacterial Canker of Kiwifruit (Pseudomonas syringae pv. actinidiae). Annual Review of Phytopathology. 2017; 1: 377–399. https://doi.org/10.1146/annurev-phyto-080516-035530

11. Renzi M, Copini P, Taddei AR, Rossetti A, Gallipoli L, Mazzaglia A, et al. Bacterial Canker on Kiwifruit in Italy: Anatomical Changes in the Wood and in the Primary Infection Sites. Phytopathology. 2012; 9: 827–840. https://doi.org/10.1094/PHYTO-02-12-0019-R PMID: 22713076

12. Serizawa S, Ichikawa T, Takikawa Y, Tsuyumu S, Goto M. Occurrence of bacterial canker of kiwifruit in Japan: description of symptoms, isolation of the pathogen and screening of bactericides. Japanese Journal of Phytopathology. 1989; 4: 427–436. https://doi.org/10.3186/jjphytopath.55.427

13. Wilstermann A, Schrader G, Kehlenbeck H, Robinet C. Potential spread of kiwifruit bacterial canker (Pseudomonas syringae pv. actinidiae) in Europe. Eppo Bulletin. 2017; 2: 255–262. https://doi.org/10.1111/epp.12385

14. Ferrante P, Scortichini M. Redefining the global populations of Pseudomonas syringae pv. actinidiae based on pathogenic, molecular and phenotypic characteristics. Plant Pathology. 2015; 1: 51–62. https://doi.org/10.1111/ppa.12236

15. Fang Y, Zhu X, Wang Y. Preliminary studies on kiwifruit diseases in Hunan Province. Sichuan Fruit Science Technology. 1990; 18: 28–29.

16. Li N, Tan GJ, Li Y, Cheng HY. Research progress and prospect on kiwifruit bacterial canker. Journal of Ahui Agricultural Sciences. 2002; 3: 391–393+401. https://doi.org/10.13989/j.cnki.0517-6611.2002.03.035

17. Zhang Y, Pang MG, Xu J, Feng H, Liu YL. Investigation and Research of Kiwifruit Actinidia bacterial (Canker). Biological Disaster Science. 2013; 1: 69–71.

18. Abelleira A, Ares A, Aguín O, Picoaga A, López MM, Mansilla P. Current situation and characterization of Pseudomonas syringae pv. actinidiae on kiwifruit in Galicia (northwest Spain). Plant Pathology. 2014; 3: 691–699. https://doi.org/10.1111/ppa.12125

19. Shao BL, Wang CH, Zhang J, Liu LX, Zhu TH, Zhuang Q. Geographical distributions of Pseudomonas syringae pv.actinidiae in China. Plant Protection. 2016; 2: 146–150.

20. Li GQ, Liu CC, Liu YG, Yang J, Zhang XS, Guo K. Advances in theoretical issues of species distribution models. Acta Ecological Sinica. 2012; 16: 4827–4835. https://doi.org/10.5846/stxb201212031735

21. Elith J, Leathwick JR. Species Distribution Models: Ecological Explanation and Prediction Across Space and Time. Annual Review of Ecology Evolution & Systematics. 2009; 1: 677–697. https://doi.org/10.1146/annurev.ecolsys.110308.120159

22. Hernandez PA, Graham CH, Master LL, Albert DL. The effect of sample size and species characteristics on performance of different species distribution modeling methods. Ecography. 2006; 5: 773–785. https://doi.org/10.1111/j.0906-7590.2006.04700.x

23. Pearson RG, Raxworthy CJ, Nakamura M, Peterson AT. ORIGINAL ARTICLE: Predicting species distributions from small numbers of occurrence records: a test case using cryptic geckos in Madagascar. Journal of Biogeography. 2007; 1: 102–117. https://doi.org/10.1111/j.1365-2699.2006.01594.x

24. Ortega-Huerta MA, Peterson AT. Modeling ecological niches and predicting geographic distributions: a test of six presence-only methods. Revista mexicana de Biodiversidad. 2008; 1: 205–216.

25. Narouei-Khandan HA, Halbert SE, Worner SP, Bruggen AHCV. Global climate suitability of citrus huanglongbing and its vector, the Asian citrus psyllid, using two correlative species distribution modeling approaches, with emphasis on the USA. European Journal of Plant Pathology. 2016; 3: 1–16. https://doi.org/10.1007/s10658-015-0804-7

26. Zhao WJ, Chen L, Ding KJ, Duan XY, Zhou YL. Prediction of potential geographic distribution areas of the maize downy mildew in China by using MAXENT. Plant Protection. 2009; 2: 32–38.

27. Cao XR, Chen L, Zhou YL, Duan XY. Potential distribution of Magnaporthe grisea in China and the world,predicted by MaxEnt. Plant Protection. 2011; 3: 80–83.

28. Zeng H, Huang G, Lin W, Liang Y, Li Z. Prediction of potential geographic distribution of Microcyclus ulei in the world using MaxEnt. Plant Protection. 2008; 3: 88–92.

29. Han Y, Wang Y, Xiang Y, Jianren YE. Prediction of potential distribution of Bursaphelenchus xylophilus in China based on Maxent ecological niche model. Journal of Nanjing Forestry University. 2015; 1: 6–10.

30. Sambaraju KR, Carroll AL, Zhu J, Stahl K, Moore RD, Aukema BH. Climate change could alter the distribution of mountain pine beetle outbreaks in western Canada. Ecography. 2012; 3: 211–223. https://doi.org/10.1111/j.1600-0587.2011.06847.x

31. Biber-Freudenberger L, Ziemacki J, Tonnang HE, Borgemeister C. Future Risks of Pest Species under Changing Climatic Conditions. Plos One. 2016; 4: e0153237. https://doi.org/10.1371/journal.pone.0153237 PMID: 27054718

32. Jo WS, Kim HY, Kim BJ. Climate change alters diffusion of forest pest: A model study. Journal of the Korean Physical Society. 2017; 1: 108–115. https://doi.org/10.3938/jkps.70.108

33. Krishnan S, Chander S. Simulation of climatic change impact on crop-pest interactions: a case study of rice pink stem borer Sesamia inferens (Walker). Climatic Change. 2015; 2: 259–272. https://doi.org/10.1007/s10584-015-1385-3

34. Ziska LH, Blumenthal DM, Runion GB, Hunt ER Jr, Diazsoltero H. Invasive species and climate change: an agronomic perspective. Climatic Change. 2011; 1: 13–42. https://doi.org/10.1007/s10584-010-9879-5

35. Romain B, Vincent P, Jean-Claude G. Disregarding the edaphic dimension in species distribution models leads to the omission of crucial spatial information under climate change: the case of Quercus pubescens in France. Global Change Biology. 2012; 8: 2648–2660.

36. Das T, Majumdar MHD, Devi RT, Rajesh T. Climate change impacts on plant diseases. SAARC Journal of Agriculture. 2017; 2: 200–209. https://doi.org/10.3329/sja.v14i2.31259

37. Schatz AM, Kramer AM, Drake JM. Accuracy of climate-based forecasts of pathogen spread. R Soc Open Sci. 2017; 3: 160975. https://doi.org/10.1098/rsos.160975 PMID: 28405387

38. Hannah L, Steele M, Fung E, Imbach P, Flint L, Flint A. Climate change influences on pollinator, forest, and farm interactions across a climate gradient. Climatic Change. 2017;: 1–13. https://doi.org/10.1007/s10584-016-1868-x

39. Franklin J, Davis FW, Ikegami M, Syphard AD, Flint LE, Flint AL, et al. Modeling plant species distributions under future climates: how fine scale do climate projections need to be? Global Change Biology. 2013; 2: 473. https://doi.org/10.1111/gcb.12051 PMID: 23504785

40. Ghini R, Hamada E, Angelotti F, Costa LB, Bettiol W. Research approaches, adaptation strategies, and knowledge gaps concerning the impacts of climate change on plant diseases. Tropical Plant Pathology. 2012; 1: 5–24. https://doi.org/10.1590/S1982-56762012000100002

41. Elad Y, Pertot I. Climate Change Impacts on Plant Pathogens and Plant Diseases. Journal of Crop Improvement. 2014; 1: 99–139. https://doi.org/10.1080/15427528.2014.865412

42. Leach K, Montgomery WI, Reid N. Modelling the influence of biotic factors on species distribution patterns. Ecological Modelling. 2016;: 96–106. https://doi.org/10.1016/j.ecolmodel.2016.06.008

43. Hijmans RJ, Graham CH. The ability of climate envelope models to predict the effect of climate change on species distributions. Global Change Biology. 2006; 12: 2272–2281. https://doi.org/10.1111/j.1365-2486.2006.01256.x

44. Butler MI, Stockwell PA, Black MA, Day RC, Lamont IL, Poulter RTM. Pseudomonas syringae pv. actinidiae from Recent Outbreaks of Kiwifruit Bacterial Canker Belong to Different Clones That Originated in China. Plos One. 2013; 2: e57464. https://doi.org/10.1371/journal.pone.0057464 PMID: 23555547

45. Ciarroni S, Gallipoli L, Taratufolo MC, Butler MI, Poulter RT, Pourcel C, et al. Development of a Multiple Loci Variable Number of Tandem Repeats Analysis (MLVA) to Unravel the Intra-Pathovar Structure of Pseudomonas syringae pv. actinidiae Populations Worldwide. Plos One. 2015; 8: 2018–2025. https://doi.org/10.1371/journal.pone.0135310 PMID: 26262683

46. Sawada H, Takeuchi T, Matsuda I. Comparative analysis of Pseudomonas syringae pv. actinidiae and pv. phaseolicola based on phaseolotoxin-resistant ornithine carbamoyltransferase gene (argK) and 16S-23S rRNA intergenic spacer sequences. Applied & Environmental Microbiology. 1997; 1: 282. PMID: 8979356

47. Ferrante P, Scortichini M. Molecular and phenotypic features of Pseudomonas syringae pv. actinidiae isolated during recent epidemics of bacterial canker on yellow kiwifruit (Actinidia chinensis) in central Italy. Plant Pathology. 2010; 5: 954–962. https://doi.org/10.1111/j.1365-3059.2010.02304.x

48. Zhao Z, Gao X, Yang D, Huang L, Qin H, Kang Z, et al. Field detection of canker-causing bacteria on kiwifruit trees: Pseudomonas syringae pv. actinidiae is the major causal agent. Crop Protection. 2015;: 55–62. https://doi.org/10.1016/j.cropro.2015.05.008

49. Tondou R, Giovanardi D, Ferrari M, Stefani E. Isolation of bacterial endophytes from Actinidia chinensis and preliminary studies on their possible use as antagonists against Pseudomonas syringae pv. actinidiae. Journal of Berry Research. 2016; 4: 1–12. https://doi.org/10.3233/JBR-160118

50. Cunty A, Poliakoff F, Rivoal C, Cesbron S, Fischer-Le Saux M, Lemaire C, et al. Characterization of Pseudomonas syringae pv. actinidiae (Psa) isolated from France and assignment of Psa biovar 4 to a de novo pathovar: Pseudomonas syringae pv. actinidifoliorum pv. nov. Plant Pathology. 2015; 3: 582–596. https://doi.org/10.1111/ppa.12297

51. Ghods S, Sims IM, Moradali MF, Rehm BHA. Bactericidal Compounds Controlling Growth of the Plant Pathogen Pseudomonas syringae pv. actinidiae, Which Forms Biofilms Composed of a Novel Exopolysaccharide. Applied & Environmental Microbiology. 2015; 12: 4026–4036. https://doi.org/10.1128/AEM.00194-15 PMID: 25841017

52. Andolfi A, Ferrante P, Petriccione M, Cimmino A, Evidente A, Scortichini M. Production of phytotoxic metabolites by Pseudomonas syringae pv. actinidiae, the causal agent of bacterial canker of kiwifruit. Plant Disease. 2011; 95: 1311. https://doi.org/10.1094/PDIS-03-11-0195

53. Vanneste JL, Yu J, Cornish DA, Tanner DJ, Windner R, Chapman JR, et al. Identification, virulence, and distribution of two biovars of Pseudomonas syringae pv. actinidiae in New Zealand. Plant Disease. 2013; 6: 708–719. https://doi.org/10.1094/PDIS-07-12-0700-RE

54. Koh YJ, Nou IS. DNA markers for identification of Pseudomonas syringae pv. actinidiae. Molecules & Cells. 2002; 2: 309–314. PMID: 12018854

55. Scortichini M. Field efficacy of chitosan to control Pseudomonas syringae pv. actinidiae, the causal agent of kiwifruit bacterial canker. European Journal of Plant Pathology. 2014; 4: 887–892. https://doi.org/10.1007/s10658-014-0515-5

56. Cameron A, Sarojini V. Pseudomonas syringae pv. actinidiae: chemical control, resistance mechanisms and possible alternatives. Plant Pathology. 2014; 1: 1–11. https://doi.org/10.1111/ppa.12066

57. López-Martínez V, Sánchez-Martínez G, Jiménez-García D, Pérez-De lO, Nidia B, Coleman TW. Environmental suitability for Agrilus auroguttatus (Coleoptera: Buprestidae) in Mexico using MaxEnt and database records of four Quercus (Fagaceae) species. Agricultural & Forest Entomology. 2016; 4: 409–418. https://doi.org/10.1111/afe.12174

58. Shrestha UB, Bawa KS. Impact of Climate Change on Potential Distribution of Chinese Caterpillar Fungus (Ophiocordyceps sinensis) in Nepal Himalaya. Plos One. 2014; 9: e106405. doi: Impact of Climate Change on Potential Distribution of Chinese Caterpillar Fungus (Ophiocordyceps sinensis) in Nepal Himalaya https://doi.org/10.1371/journal.pone.0106405 PMID: 25180515

59. Remya K, Ramachandran A, Jayakumar S. Predicting the current and future suitable habitat distribution of Myristica dactyloides Gaertn. using MaxEnt model in the Eastern Ghats, India. Ecological Engineering. 2015; 9: 184–188. https://doi.org/10.1016/j.ecoleng.2015.04.053

60. Petersen MJ. Evidence of a climatic niche shift following North American introductions of two crane flies (Diptera; genus Tipula). Biological Invasions. 2013; 4: 885–897. https://doi.org/10.1007/s10530-012-0337-3

61. Gelviz-Gelvez SM, Pavón NP, Illoldi-Rangel P, Ballesteros-Barrera C. Ecological niche modeling under climate change to select shrubs for ecological restoration in Central Mexico. Ecological Engineering. 2015;: 302–309. https://doi.org/10.1016/j.ecoleng.2014.09.082

62. Jiang HJ, Liu T, Li L, Zhao Y, Pei L, Zhao JC. Predicting the Potential Distribution of Polygala tenuifolia Willd. under Climate Change in China. Plos One. 2016; 9: e0163718. https://doi.org/10.1371/journal.pone.0163718 PMID: 27661983

63. Zhang L, Cao B, Bai C, Li G, Mao M. Predicting suitable cultivation regions of medicinal plants with Maxent modeling and fuzzy logics: a case study of Scutellaria baicalensis in China. Environmental Earth Sciences. 2016; 5: 361. https://doi.org/10.1007/s12665-015-5133-9

64. Choudhury MR, Deb P, Singha H, Chakdar B, Medhi M. Predicting the probable distribution and threat of invasive Mimosa diplotricha Suavalle and Mikania micrantha Kunth in a protected tropical grassland. Ecological Engineering. 2016; December: 23–31. https://doi.org/10.1016/j.ecoleng.2016.07.018

65. Worthington TA, Zhang T, Logue DR, Mittelstet AR, Brewer SK. Landscape and flow metrics affecting the distribution of a federally-threatened fish: Improving management, model fit, and model transferability. Ecological Modelling. 2016;: 1–18. https://doi.org/10.1016/j.ecolmodel.2016.09.016

66. Phillips SJ, Anderson RP, Schapire RE. Maximum entropy modeling of species geographic distributions. Ecological Modelling. 2006; 3–4: 231–259. https://doi.org/10.1016/j.ecolmodel.2005.03.026

67. Bradie J, Leung B. A quantitative synthesis of the importance of variables used in MaxEnt species distribution models. Journal of Biogeography. 2017;: https://doi.org/10.1111/jbi.12894

68. Kumar S, Yee WL, Neven LG. Mapping Global Potential Risk of Establishment of Rhagoletis pomonella (Diptera: Tephritidae) Using MaxEnt and CLIMEX Niche Models. Journal of Economic Entomology. 2016; 5: tow166. https://doi.org/10.1093/jee/tow166 PMID: 27452001

69. Penado A, Rebelo H, Goulson D. Spatial distribution modelling reveals climatically suitable areas for bumblebees in undersampled parts of the Iberian Peninsula. Insect Conservation & Diversity. 2016; 5: 391–401. https://doi.org/10.1111/icad.12190

70. Bosso L, Febbraro MD, Cristinzio G, Zoina A, Russo D. Shedding light on the effects of climate change on the potential distribution of Xylella fastidiosa in the Mediterranean basin. Biological Invasions. 2016; 6: 1759–1768. https://doi.org/10.1007/s10530-016-1118-1

71. Rameshprabu N, Swamy PS. Prediction of environmental suitability for invasion of Mikania micrantha in India by species distribution modelling. Journal of Environmental Biology. 2015; 3: 565–570.

72. Peterson AT, Pape M, f x, Eaton M. Transferability and model evaluation in ecological niche modeling: a comparison of GARP and Maxent. Ecography. 2007; 4: 550–560. https://doi.org/10.1111/j.0906-7590.2007.05102.x

73. Quenouille MH. Approximate Tests of Correlation in Time-Series. Journal of the Royal Statistical Society. 1949; 1: 68–84. https://doi.org/10.1017/S0305004100025123

74. Tukey JW. Bias and Confidence in Not Quite Large Samples. Annals of Mathematical Statistics. 1958; 2: 614. https://doi.org/10.1214/aoms/1177706647

75. Yue TX, Fan ZM, Chen CF, Sun XF, Li BL. Surface modelling of global terrestrial ecosystems under three climate change scenarios. Ecological Modelling. 2011; 14: 2342–2361. https://doi.org/10.1016/j.ecolmodel.2010.11.026

76. Elith J, Yates CJ. A statistical explanation of MaxEnt for ecologists. Diversity & Distributions. 2011; 1: 43–57.

77. Sobekswant S, Kluza DA, Cuddington K, Lyons DB. Potential distribution of emerald ash borer: What can we learn from ecological niche models using Maxent and GARP? Forest Ecology & Management. 2012; 4: 23–31. https://doi.org/10.1016/j.foreco.2012.06.017

78. Qin Z, Zhang JE, Ditommaso A, Wang RL, Wu RS. Predicting invasions of Wedelia trilobata (L.) Hitchc. with Maxent and GARP models. Journal of Plant Research. 2015; 5: 1–13. https://doi.org/10.1007/s10265-015-0738-3

79. Cai JY, Zhang MM, Su HJ, Zhang HB. Application of Ecological Niche Models for Selection of Species Habitat. Journal of EConomic Animal. 2014; 1: 47–52. https://doi.org/10.13326/j.jea.2014.0012

80. Yi YJ, Cheng X, Yang ZF, Zhang SH. Maxent modeling for predicting the potential distribution of endangered medicinal plant (H. riparia Lour) in Yunnan, China. Ecological Engineering. 2016;: 260–269. https://doi.org/10.1016/j.ecoleng.2016.04.010

81. Yang XQ, Kushwaha SPS, Saran S, Xu J, Roy PS. Maxent modeling for predicting the potential distribution of medicinal plant, Justicia adhatoda L. in Lesser Himalayan foothills. Ecological Engineering. 2013; 1: 83–87. https://doi.org/10.1016/j.ecoleng.2012.12.004

82. Merow C, JAS Jr. A comparison of Maxlike and Maxent for modelling species distributions. Methods in Ecology & Evolution. 2014; 3: 215–225. https://doi.org/10.1111/2041-210X.12152

83. Dormann CF, Singer A. Correlation and process in species distribution models: bridging a dichotomy. Journal of Biogeography. 2012; 12: 2119–2131. doi: Correlation and process in species distribution models: bridging a dichotomy

84. David H. A statistical explanation of MaxEnt for ecologists. Diversity and Distributions. 2013; 1: 43–57. https://doi.org/10.1111/j.1472-4642.2010.00725.x

85. Morán-Ordóñez A, Lahoz-Monfort JJ, Elith J, Wintle BA. Evaluating 318 continental-scale species distribution models over a 60-year prediction horizon: what factors influence the reliability of predictions? Global Ecology & Biogeography. 2016; 3: 371–384. https://doi.org/10.1111/geb.12545

86. Breiner FT, Guisan A, Bergamini A, Nobis MP. Overcoming limitations of modelling rare species by using ensembles of small models. Methods in Ecology & Evolution. 2015; 10: 1210–1218. https://doi.org/10.1111/2041-210X.12403

87. Sivaraj N, Elangovan M, Kamala V, Pandravada SR, Pranusha P, Chakrabarty SK. Maximum Entropy (Maxent) Approach to Sorghum Landraces Distribution Modelling. 2016; 1: 16. https://doi.org/10.5958/0976-1926.2016.00004.8

88. Fand BB, Kumar M, Kamble AL. Predicting the potential geographic distribution of cotton mealybug Phenacoccus solenopsis in India based on MAXENT ecological niche model. J Environ Biol. 2014; 5: 973–982. PMID: 25204075

89. Kalle R, Ramesh T, Qureshi Q, Sankar K. Predicting the distribution pattern of small carnivores in response to environmental factors in the Western Ghats. Plos One. 2013; 11: e79295. https://doi.org/10.1371/journal.pone.0079295 PMID: 24244470

90. Thakur MP, Tilman D, Purschke O, Ciobanu M, Cowles J, Isbell F, et al. Climate warming promotes species diversity, but with greater taxonomic redundancy, in complex environments. Science Advances. 2017; 7: e1700866. https://doi.org/10.1126/sciadv.1700866

91. Serizawa S, Ichikawa T. Epidemiology of bacterial canker of kiwifruit. 2. The most suitable times and environments for infection on new canes. Japanese Journal of Phytopathology. 1993; 4: 460–468. https://doi.org/10.3186/jjphytopath.59.460

92. Li YZ, Song XB, Zhang XW. Sutdies on laws of occurrence of bacterial canker in kwifruit. Journal of Northwest Forestry University. 2000; 2: 53–56.